Figure 1 (abstract O43)

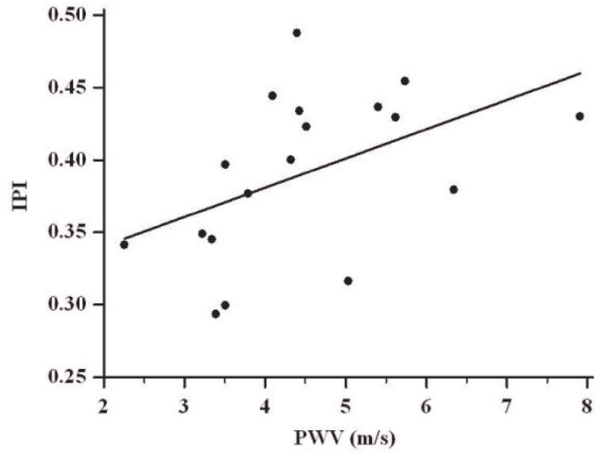

regional (aortic distensibility) aortic stiffness. Assessment can be combined with precise measurement of carotid atheroma burden, a marker of early sub-clinical atherosclerosis. We investigated whether aortic stiffness in early adult life is already associated with early changes in carotid structure.

Purpose: To determine whether aortic stiffness – quantified by cardiovascular magnetic resonance as pulse wave velocity (PWV) and aortic distensibility (AD) – is associated with early atherosclerosis-related structural changes in young adult life.

Methods: Thirty young healthy volunteers (aged 23–33) (without history of cardiovascular disease or classical risk factors for atherosclerosis) underwent CMR for measurement of aortic function and carotid wall imaging.

Aortic distensibility was measured from breath-hold ECG-gated, steady state free precession (SSFP) images. Distensibility was calculated as the relative change in area divided by the central pulse pressure. Pulse wave velocity was measured from an ECG-gated, free breathing, spoiled gradient echo phase-encoded acquisition. The transit time method was used for the calculation of pulse wave velocity (PWV). T1 weighted black blood turbo spin echo (TSE) cross-sectional images of both carotid arteries, centred at the lowest bifurcation were used for atheroma burden measurements (plaque index represented cross-sectional vessel wall area/total cross-sectional vascular area). Plaque index was averaged for the common carotid (CPI), the carotid bulb (BPI) and the internal carotid artery (IPI).

Results: CMR-derived PWV over the whole length of the aorta was correlated with carotid plaque index ($r = 0.480$, $P < 0.05$) (Figure 1.) particularly of the internal carotid artery. Regional measures of aortic distensibility and pulse wave velocity were unrelated to carotid atheroma burden. Applying a multiple regression analysis model (including applicable risk factors, demographics and anthropometric measurements) PWV was the sole independent predictor of IPI [$\beta = 0.02(\pm 0.009)$, $P < 0.05$, $R^2 = 0.23$].

Conclusion: Aortic stiffness assessed by CMR is associated with early atherosclerosis-related changes in carotid arteries in young adults.

O44

Relationship between regional wall shear stress and carotid plaque composition using 3 T MRI and patient-specific computational fluid dynamics

Raymond Q Migrino[1], Mark Bowers[1], Leanne Harmann[1], Robert Prost[1], Anil Doppalapudi[1], Tayyab Mohyuddin[1], Megan Bright[1], Jason Jurva[1], Osama Zaidat[1] and John LaDisa[2]

[1]*Medical College of Wisconsin, Milwaukee, WI, USA*
[2]*Marquette University, Milwaukee, WI, USA*

Journal of Cardiovascular Magnetic Resonance 2009, **11(Suppl 1):**O44

Introduction: Plaque vulnerability arises from the interplay among factors including plaque composition (PC) and wall shear stress (WSS). To date, the relationship between spatial WSS and PC is not established.

Purpose: Our aim is to determine the relationship between WSS and PC in established carotid atherosclerosis.

Methods: 5 subjects (4 males, 66 ± 8 years), with moderate to severe carotid plaque underwent 3 T MRI using 4-channel carotid coil. T1, T2, proton density and time of flight images were obtained (0.47–0.55 × 0.47–0.55 × 2 mm spatial resolution) 12 mm above and below the bifurcation. Plaque composition (necrotic core and loose matrix) were quantified using Plaque-view software (VP Diagnostics). Subject-specific computational fluid dynamic models were created from MRI, B-mode ultrasound and blood pressure (BP) data using CVsim software. Outlet boundary conditions that replicated flow and BP were applied and simulations used a stabilized finite element solver. Each carotid slice were divided into 6 circumferential regions where WSS was correlated with PC.

Results: Please see figure 1. WSS correlated significantly with necrotic core ($R = 0.283$, $p < 0.001$) but not with loose matrix ($R = -0.03$, $p = 0.6$). The same relationship was seen in the common carotid, bifurcation or internal carotid artery. Carotid plaque regions with necrotic core had higher WSS than those without (34.1 ± 2.6 vs. 17.3 ± 4.6 dyn/cm^2, $p < 0.001$). WSS in regions with and without loose matrix did not differ (25.8 ± 3.6 vs. 22.5 ± 3.3, $p = 0.7$).

Conclusion: In established carotid artery disease, regions with high WSS are associated with increased necrotic core, but not

Figure 1 (abstract O44)

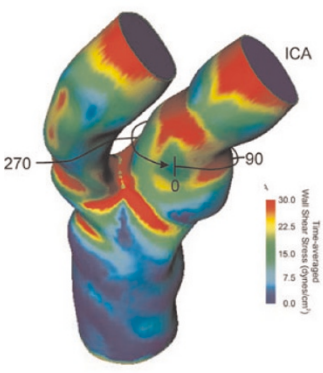

CFD Model and Regional WSS

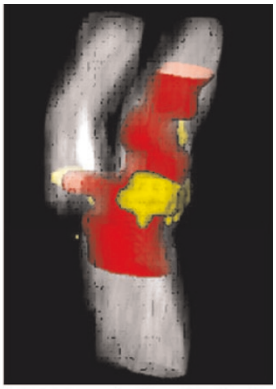

MRI: Necrotic Core (Yellow), Blood Pool (Red)

loose matrix. This relationship between increased WSS and necrotic core content in the plaque may play an important role in plaque vulnerability.

O45
A novel, dual-contrast in-vivo MR imaging method with principal component analysis reliably quantifies lipid-rich necrotic core and collagen in human carotid atherosclerotic plaques

Zhen Qian, Sarah Rinehart, Laura J Murrieta, Gustavo Vasquez, Patrick M Battey and Szilard Voros
Piedmont Heart Institute, Atlanta, GA, USA

Journal of Cardiovascular Magnetic Resonance 2009, **11(Suppl 1):**O45

Background: In-vivo multi-spectral imaging of human carotid plaques using different pulse sequences, with and without exogenous contrast agents, has been implemented. However, an in-vivo dual-contrast approach with small paramagnetic iron oxide (SPIO) and gadolinium at multiple timepoints with principal component analysis (PCA) has not been previously performed.
Purpose: To develop a novel, PCA-based method for the detection of lipid-rich necrotic core (LRNC) and collagen in human carotid plaques utilizing a dual-contrast approach. We hypothesized that LRNC and collagen can be reliably identified based on different signal characteristics with different exogenous contrast agents and multiple different imaging pulse sequences.
Methods: 10 pts scheduled for carotid endarterectomy (CEA) were imaged at 1.5 T with a dedicated small surface coil. T1, T2 and inversion recovery delayed hyperenhancement (DHE) images with magnitude/phase reconstruction were obtained before contrast, immediately and 24 hours after 0.05 cc/kg of SPIO (Feridex) and after 30 cc of Gd. Imaging parameters were: T1; TR: 1500 ms, TE 10 ms, slice 3 mm, matrix 320 × 320, averages 3; T2; TR: 2500 ms, TE 92 ms, slice 3 mm, matrix 320 × 320, averages 4; DHE; TR: 745 ms, TE 3.5 ms, slice 6 mm, matrix 192 × 192, averages 1. Corresponding histological sections from CEA specimens were stained with Movat's pentachrome for identification of LRNC and collagen.
For a training dataset, ROI in two pts were normalized to foreground median intensity and histopathological specimens were non-rigidly registered to the MR images using anatomical landmarks and a thin-plate spline-based image morphing algorithm (Panel C). Plaque composition masks consisting of 6 classes (LRNC [red], calcium [yellow], fibrous collagen [green], proteoglycans [light blue], elastin [grey], and fibrin [purple]) were created based on the registered histological images (Panel D). All 4 sequences at all 4 timepoints were independently tested for the identification of plaque composition. A more comprehensive PCA analysis utilizing all pulse sequences at all timepoints was also performed. Signal intensity (SI) statistics are expressed as mean ± SD. The performance of composition identification was measured by comparing the predicted compositions with the 2-class mask, and was evaluated using the two-tailed t-test p value, and the area under the ROC curve.
Results: See Figure 1. SI was significantly higher in LRNC on T2 images immediately after SPIO (Panel A) compared to other tissues (56.66 ± 18.52 vs. 26.21 ± 12.74, $p < 0.0001$). PCA showed significant difference between LRNC and non-LRNC tissue ($p < 0.0001$) (Panel E). The percentage of correctly identified pixels was 80.4%. Predicted total area for LRNC was 71 pixels (22.22 mm^2), compared to 66 pixels (20.65 mm^2) on the manually identified mask (Panel F, G). ROC curve analysis showed that PCA (AUC: 0.96) was significantly better than the single best approach (T2 immediately post-SPIO; AUC: 0.90) ($p = 0.016$) (Panel H).

Figure 1 (abstract O45)

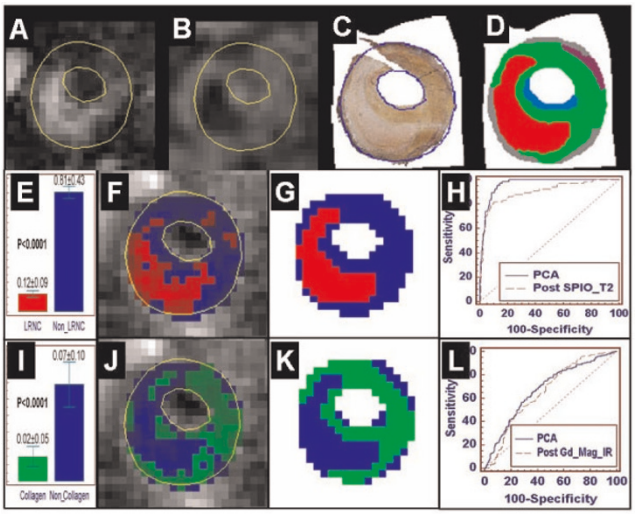

SI was significantly higher in collagen on the post-Gd DHE magnitude images (Panel B) (36.56 ± 8.97 vs. 30.21 ± 12.80, $p < 0.0001$). PCA showed significant difference between collagen and non-collagen tissue ($p < 0.0001$) (Panel I). The percentage of correctly identified pixels was 65.8%. Predicted total area for collagen was 104 pixels (32.54 mm^2), compared to 98 pixels (30.67 mm^2) on the manually identified mask (Panel J, K). ROC curve analysis showed that PCA (AUC: 0.68) was similar to the single best approach (Post-Gd magnitude DHE; AUC: 0.66) ($p = 0.562$) (Panel L).
Conclusion: LRNC and collagen can be reliably identified in-vivo in human carotid atherosclerotic plaques using our novel, dual-contrast approach; a different pulse sequence with different exogenous contrast is optimal for the identification of different tissue components. A more sophisticated PCA analysis is significantly better than the evaluation of a single pulse sequence at a single timepoint for the identification of LRNC. Such sophisticated plaque analysis can now be applied to clinical outcomes studies and for the evaluation of the effects of pharmaceutical agents for the modification of atherosclerosis.

O46
In vivo human coronary magnetic resonance angiography at 7 Tesla

Saskia GC van Elderen[1], Andrew G Webb[1], Maarten Versluis[1], Jos Westenberg[1], Joost Doornbos[1], Nadine B Smith[1], Albert de Roos[1] and Matthias Stuber[2]
[1]*LUMC, Leiden, Netherlands*
[2]*John Hopkins University, Baltimore, MD, USA*

Journal of Cardiovascular Magnetic Resonance 2009, **11(Suppl 1):**O46

Introduction: Coronary magnetic resonance angiography (MRA) is a promising technique for the non-invasive visualization